Available online at www.sciencedirect.com
ScienceDirect
Polymer 47 (2006) 6773–6781
polymer
www.elsevier.com/locate/polymer

Achievement of quasi-nanostructured polymer blends by solid-state shear pulverization and compatibilization by gradient copolymer addition

Ying Tao [a], Jungki Kim [a], John M. Torkelson [a,b,*]

[a] Department of Chemical and Biological Engineering, Northwestern University, 2145 Sheridan Road, Evanston, IL 60208-3120, USA
[b] Department of Materials Science and Engineering, Northwestern University, 2145 Sheridan Road, Evanston, IL 60208-3120, USA

Received 8 June 2006; received in revised form 20 July 2006; accepted 21 July 2006
Available online 14 August 2006

Abstract

Nanoblends, in which dispersed-phase domains exhibit length scales of order 100 nm or less, are made using a continuous, industrially scalable, mechanical process called solid-state shear pulverization (SSSP). An 80/20 wt% polystyrene (PS)/poly(methyl methacrylate) (PMMA) blend processed by SSSP and consolidated by platen pressing, without melt processing, exhibits a quasi-nanostructured morphology with many irregular, minor-phase domain sizes of ~100 nm or less. After short-residence-time single-screw extrusion, the pulverized blend exhibits spherical dispersed-phase domains with a number-average diameter of 155 nm. Thus, SSSP followed by certain melt-processing operations can yield nanoblends. However, the pulverized blend exhibits significant coarsening of the dispersed-phase domains during long-term, high-temperature static annealing, indicating that SSSP followed by other melt processes may yield microstructured blends. In order to suppress coarsening, a styrene (S)/methyl methacrylate (MMA) gradient copolymer is synthesized by controlled radical polymerization. When 5 wt% S/MMA gradient copolymer is added to the PS/PMMA blend during SSSP, the resulting blend exhibits a nanostructure nearly identical to that of the blend without gradient copolymer, and coarsening is nearly totally suppressed during long-term, high-temperature static annealing. Thus, SSSP with gradient copolymer addition can yield compatibilized nanoblends. Morphologies obtained in the pulverized PS/PMMA nanoblend are compared with those in blends of PS/poly(*n*-butyl methacrylate) and PS/high-density polyethylene made using identical SSSP conditions, providing for commentary on the ability of SSSP to produce nanostructured blends as a function of blend components.

Keywords: Nanoblend; Solid-state shear pulverization; Gradient copolymers

1. Introduction

The achievement of nanostructured blends of thermoplastic polymers, which are often called nanoblends, is of recent growing interest [1–23] because these materials have the potential for enhanced properties (e.g., transparency, heat resistance, creep resistance, etc.) in comparison with conventional immiscible polymer blends with average dispersed-phase sizes on the micron scale. Many of the previous studies have emphasized nanoblend production, i.e., the production of an immiscible blend in which one of more of the phase domains is of order 100 nm or less in length scale, via in situ polymerization of one monomer in the presence of another polymer or by reactive blending [2,6,8,11–13,18–20,22]. For example, Alam et al. [22] prepared quasi-nanostructured blends by in situ ring-opening polymerization of macrocyclic carbonates in the presence of a maleic anhydride-modified polypropylene matrix. Also, Leibler and co-workers [8,20] have produced co-continuous nanostructured polyethylene/polyamide blends by reactive melt blending in which irregular graft copolymers were made in situ.

Here we limit our focus to the production of nanostructured blends with processes that rely neither on in situ polymerization nor on reactive blending. One option is the production of nanoblends via melt processing, e.g., extrusion. However, there are limitations regarding the dispersed-phase domain size that may be achieved in blends with conventional melt

* Corresponding author. Department of Chemical and Biological Engineering, Northwestern University, 2145 Sheridan Road, Evanston, IL 60208-3120, USA.
E-mail address: j-torkelson@northwestern.edu (J.M. Torkelson).

0032-3861/$ - see front matter © 2006 Published by Elsevier Ltd.
doi:10.1016/j.polymer.2006.07.041

processes. When an immiscible blend consisting of major and minor phases is melt mixed, the dispersed-phase polymer pellets or flakes are generally first deformed into sheets; this may be followed by the formation of filaments which subsequently break into droplets and are then further deformed and broken into smaller domains. The droplet breakup is repeated until the interfacial stress of the dispersed domains can withstand the stress of the imposed flow. Competing with dispersed-phase droplet breakup is droplet coalescence (or, more correctly, coarsening if both coalescence and Ostwald ripening effects are present) in which two droplets combine to form one larger droplet with a net reduction in interfacial area. Coalescence is a major stumbling block associated with the melt-state production of immiscible polymer blends with small dispersed-phase domains. As a result, many different strategies have been investigated in an attempt to suppress coalescence and thereby compatibilize polymer blends [24]. In certain cases, addition of large levels of block copolymer (e.g., 15–30 wt% styrene/ethylene–butylene/styrene) to a blend with a low level of a dispersed phase (90/10 wt% polystyrene/ethylene–propylene rubber) has allowed the production of immiscible blends with dispersed-phase domains having average diameters of 300–400 nm [25]. A full description of morphological development during liquid-state processing of polymer blends is beyond the scope of this manuscript; relevant discussion may be found in Refs. [26–34].

Shimizu et al. [21] have recently demonstrated that nanoblends can be made by melt-state processing without the use of added block copolymer. They employed an innovative, unconventional high-shear extruder with an extremely small length-to-diameter ratio of 1.78 and shear rates exceeding 1000 s^{-1}. The unusually high-shear rates associated with their apparatus, which are an order of magnitude greater than those using conventional extruders, yielded sub-100 nm diameters of dispersed-phase polyamide 11 in poly(vinylidene fluoride).

We have chosen to investigate the production of nanoblends via a solid-state processing method that relies neither on in situ polymerization nor on reactive blending. A number of solid-state or mechanical processing methods have been investigated for the production of immiscible polymer blends, including ball milling [4,5,35–38] and pan milling [39]. A disadvantage of these approaches is that they are batch processes. Here we employ solid-state shear pulverization (SSSP), a continuous, industrially scalable process that involves the use of equipment resembling a modified twin-screw extruder but with processing at room temperature or below. During SSSP, the polymer is exposed to high compressive and shearing forces, resulting in repeated fragmentation and fusion of the material and leading to dispersion. The SSSP process has been used previously to produce microscale polymer blends [40–48], which in some cases have been compatibilized by in situ production of block copolymer [44,45] or by the addition of block copolymer to the blend during SSSP [47].

Here we demonstrate that a nanostructured morphology can be achieved by SSSP of an 80/20 wt% polystyrene (PS)/poly(methyl methacrylate) (PMMA) blend. Nanostructured morphologies are present in the SSSP output, which is a powdery particulate, and when the SSSP output is melt processed by short-residence-time single-screw extrusion. While both the SSSP output and the extruder output of the pulverized blend are nanostructured, the SSSP output exhibits irregular, non-spherical dispersed domains with some indication of co-continuity while the extruder output exhibits largely spherical, dispersed nanodomains. We also demonstrate that compatibilized PS/PMMA nanoblends, in which coalescence is suppressed even during long-term high-temperature annealing, can be produced by the addition of 5 wt% styrene (S)/methyl methacrylate (MMA) gradient copolymer to the blend during SSSP. Gradient copolymers, which are made by simple, inexpensive controlled radical polymerization (CRP), are a novel class of polymers that have a composition gradient along the chain length [49–57] and are expected to have much higher critical micelle concentrations and better interfacial properties than block copolymers [58–60] that are added to blends. We have recently shown that gradient copolymers are highly effective in compatibilizing microstructured polymer blends when added at low levels to blends during melt mixing [53,55]. Finally, by comparing morphologies obtained in PS/PMMA, PS/poly(*n*-butyl methacrylate) (PnBMA) and PS/high-density polyethylene (HDPE) blends using constant SSSP process conditions, we comment on the possible effects of polymer properties on the achievement of nanostructures in a broad range of blends via SSSP.

2. Experimental

2.1. Materials

Polystyrene was from BASF (polystyrol pellets; M_n = 116,000 g/mol, M_w = 280,000 g/mol, determined by gel permeation chromatography (GPC; Waters Breeze) relative to PS standards). Poly(methyl methacrylate) was from Atohaas (pellets; M_n = 54,000 g/mol, M_w = 100,000 g/mol, determined by GPC using universal calibration in conjunction with PS standards in tetrahydrofuran (THF)). Poly(*n*-butyl methacrylate) was from Aldrich (powder; M_w = 337,000 as reported by the supplier). Styrene and MMA were from Aldrich and were deinihibited using inhibitor remover (Aldrich) and dried over CaH_2 before use. The unimolecular initiator alkoxyamine 29 (2,2,5-trimethyl-3-(1-phenylethoxy)-4-phenyl-3-azahexane) [61], the same as that synthesized in Ref. [53], was used in synthesizing S/MMA gradient copolymer.

2.2. Synthesis and characterization of S/MMA gradient copolymer

A semi-batch, nitroxide-mediated CRP of S and MMA was employed for the S/MMA gradient copolymer synthesis. In a round bottom flask, S (70 ml; 0.61 mol) was combined with alkoxyamine 29 (4.8×10^{-3} mol/l), and the flask was sealed using a rubber septum. A needle was inserted to blow dry N_2 into the reaction flask. Following a 30 min N_2 purge, polymerization was started by placing the flask in an oil bath (93 °C) while a syringe pump was delivering MMA into the reaction flask (flow

rates of MMA: 10 ml/h for the initial 3 h, 15 ml/h for the middle 3 h, and 20 ml/h for the last 3 h). Aliquots (~0.5 ml) of the reaction mixture were collected every 2 h during polymerization and precipitated into methanol in order to analyze the apparent molecular weight and cumulative styrene mole fraction (F_S) in each copolymer. The semi-batch copolymerization was performed for 9 h under N_2 atmosphere, and the resulting S/MMA gradient copolymer was washed via several cycles of dissolution in THF and precipitation into excess methanol. The powdery copolymer was isolated by filtering and dried at room temperature for a day followed by drying under vacuum at 70–80 °C for a second day.

The relative integral values from ^{1}H NMR spectra (Varian Inova 500 MHz; $CDCl_3$) corresponding to benzyl H's (5H from styrene; 6.2–7.2 ppm) and to all other H's (3H from styrene and 8H from methyl methacrylate; 0.6–3.6 ppm) were analyzed to determine F_S of each intermediate aliquot and the final S/MMA gradient copolymer (SgradMMA). The 'apparent' molecular weight (relative to the calibration using PS standards in THF) of each intermediate and final copolymer was obtained from GPC.

2.3. Processing

The PS/PMMA, PS/PMMA/SgradMMA, and PS/PnBMA blends were initially dry blended and then processed by SSSP using a Berstorff PT-25 twin-screw pulverizer with a screw diameter of 25 mm and a length-to-diameter ratio of 26.5. Details on the pulverizer and associated chiller unit can be found in Refs. [42,62]. All pulverization was done with the ethylene glycol/water mix used for coolant maintained at a temperature of −7 °C and a screw speed of 300 rpm. The screw design consisted of conveying elements immediately below the hopper, two bi-lobe elements (conventional mixing elements used in twin-screw extrusion), more conveying elements, and seven tri-lobe elements (referred to pulverization elements) just prior to output. Both bi-lobe and tri-lobe elements can be described as forward, reverse (providing back flow), or neutral. The two bi-lobe elements were forward elements, while the tri-lobe elements consisted of four forward, two neutral, and one reverse.

Pulverized PS/PMMA, PS/PMMA/SgradMMA, and PS/PnBMA blends were then consolidated by short-residence-time single-screw extrusion (Randcastle Extrusion Systems, Inc. RC 0625; die temperature = 200 °C). These blends were also subjected to static high-temperature annealing at 190 °C for 10 and 60 min using a differential scanning calorimeter (Mettler-Toledo DSC 822e). For purposes of comparison, PS/PMMA and PS/PnBMA blends were also made by melt mixing in a cup and rotor mixer (Atlas Polymer Evaluation Products LMM Laboratory Mixing Molder) at 210 °C for 10 min. In order to optimize mixing efficiency, three steel balls were added to the cup prior to mixing, following the protocol in Ref. [63].

2.4. Sample preparation and morphological analysis

Both PS/PMMA and PS/PnBMA pulverized outputs, which were in the form of powders, were cold pressed using a platen press (Farrel 100 ton Hydraulic Laboratory Press) at room temperature to form sample disks. For the purposes of scanning electron microscopy (SEM), samples were fractured by cutting sample disks in liquid N_2 using razor blades. Acetic acid was used to wash away the PMMA phase in the fractured surface of a PS/PMMA blend. 2-Propanol was used to wash away the PnBMA phase in the fractured surface of a PS/PnBMA blend. The fractured surfaces were then coated with a ~3.5-nm layer of gold using a Cressington 208HR high-resolution coater in order to minimize sample charging effects due to the electron beam. In order to characterize the blends with nanostructured morphologies, a high-resolution field-emission scanning electron microscope (Hitachi S4500 equipped with a cold field-emission gun) was employed with a 2 kV accelerating voltage. A conventional scanning electron microscope (Hitachi S3500) equipped with a thermal emission gun was used to observe microstructured morphologies. Scion Image Beta 4.0.2 image analysis software was used to determine the number-average dispersed-phase diameter, D_n, from the calculation of the area of ~300 particles.

2.5. Molecular weight characterization of pulverized PS/PMMA blend

The M_n and M_w values of each polymer were characterized by GPC relative to PS standards in THF. In order to measure the molecular weight of PS in a pulverized PS/PMMA blend, a dilute solution of the blend in THF was injected into the GPC. An ultraviolet absorbance detector with wavelength set at 254 nm was employed because PS absorbs strongly and PMMA absorbs negligibly at that wavelength. In order to measure the molecular weight of PMMA in a pulverized PS/PMMA blend, the PMMA was first extracted from the blend by use of acetic acid, in which PMMA is soluble and PS is totally insoluble. A dilute solution of the recovered PMMA in THF was injected into the GPC, with detection of the PMMA by refractive index.

3. Results and discussion

Fig. 1 compares the morphologies of 80/20 wt% PS/PMMA blends prepared by SSSP with those prepared by melt mixing in a minimax mixer (with three steel balls added to the mixer in order to optimize mixing as described in Ref. [63]). The pulverized blend resulted in a powdery particulate product that was subjected to room-temperature pressing via a platen press to form a fully consolidated sample. Thus, the sample shown in Fig. 1a was not subjected to any processing above the glass transition temperatures (T_gs) of the polymers constituting the blend. As a result, an unusual morphology for a blend is obtained in the pulverized sample, which involves a 3D irregular structure with some indications of co-continuity. When the blend is glassy, the dispersed-phase PMMA domains are not impacted by interfacial tension effects; thus, it is reasonable for such an irregular morphology to be achieved after the numerous repeated fragmentation and fusion steps involved in SSSP. In contrast, the blend made by melt mixing

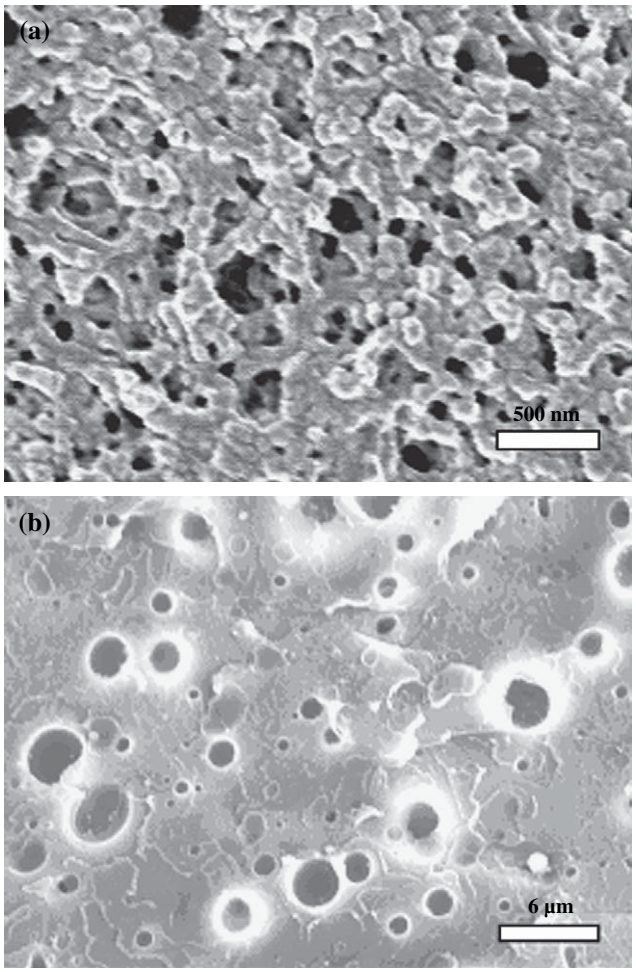

Fig. 1. Scanning electron micrographs of an 80/20 wt% PS/PMMA blend prepared via (a) SSSP followed by platen pressing without melt processing and then extraction of PMMA by acetic acid (size bar = 500 nm), and (b) melt mixing in a minimax mixer with three steel balls and then extraction of PMMA by acetic acid (size bar = 6 μm).

exhibits spherical dispersed-phase domains; this is due to the impact of interfacial tension in melt-state materials leading to dispersed-phase domains of minimal interfacial area.

Another striking difference between the blends made by SSSP and by melt mixing is the size of the dispersed-phase domains. Most of the dispersed-phase domain sizes observed in the melt-mixed blend are ~1 μm, which is a common length scale for dispersed-phase domains in PS/PMMA blends made by melt mixing [53,64,65]. However, in the case of the PS/PMMA blend made by SSSP, the dispersed-phase PMMA domain sizes are ~100 nm, an order of magnitude smaller than those obtained in the melt-mixed samples. The production of nanostructured blends or nanoblends via SSSP is significantly associated with the fact that SSSP eliminates key limitations associated with melt mixing of blends, such as interfacial tension effects and mismatched viscosities. Thus, if the many repeated fragmentation and fusion steps associated with SSSP occur under appropriate conditions for a particular polymer blend, it is possible for SSSP to yield dramatically improved dispersion of a minor polymer phase in a major polymer phase as compared with melt mixing.

Because final products made from thermoplastic blends generally involve a melt-processing stage, a concern associated with the production of nanoblends by SSSP is whether the nanoscale dispersed phase is maintained during melt processing. Comparison of Figs. 1a and 2a shows how the nanostructure obtained in the 80/20 wt% PS/PMMA blend made by

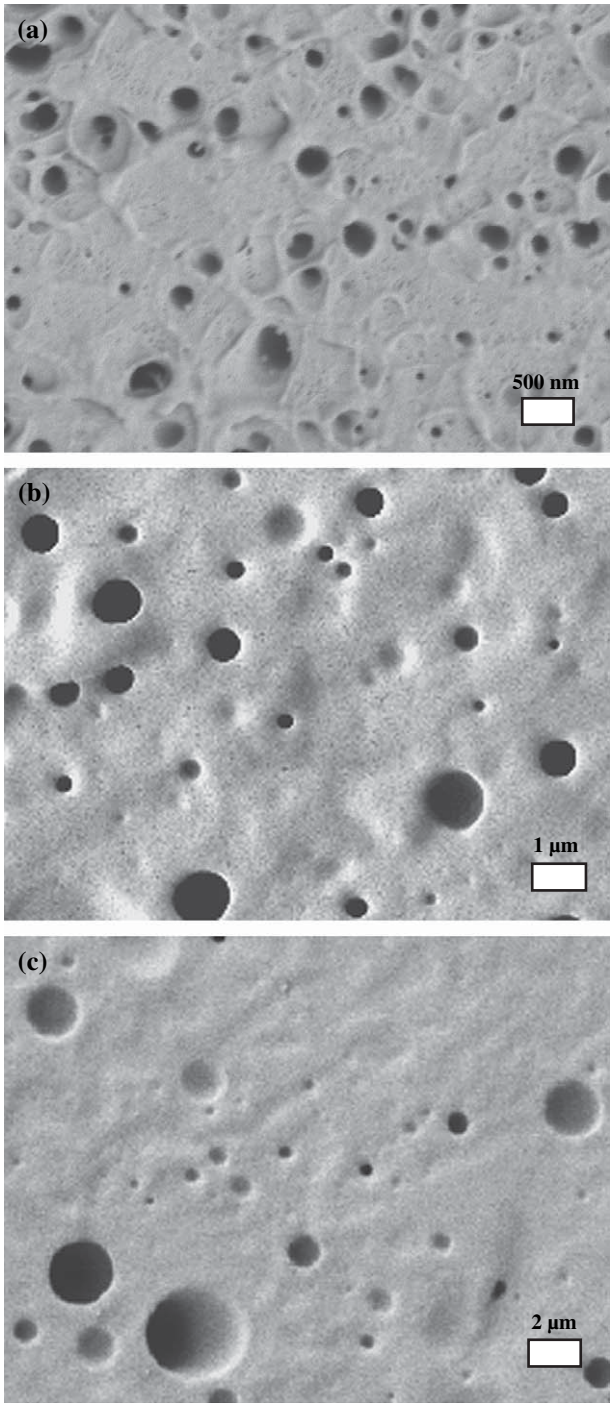

Fig. 2. Scanning electron micrographs of 80/20 wt% PS/PMMA blends prepared via SSSP followed by (a) single-screw melt extrusion (size bar = 500 nm), (b) single-screw melt extrusion and static annealing at 190 °C for 10 min (size bar = 1 μm), and (c) single-screw melt extrusion and static annealing at 190 °C for 60 min (size bar = 2 μm). In each case, PMMA was extracted using acetic acid.

SSSP is modified by processing in a short-residence-time single-screw extruder with a 200 °C die temperature. After single-screw extrusion, the vast majority of the PMMA dispersed-phase domains are observed to have 50–200 nm diameters, and image analysis of the dispersed-phase particles yields a number-average dispersed-phase domain diameter, D_n, of 155 nm (estimated error of ±10 nm). (We note that the etching technique employed in the present study involving the washing away of the PMMA dispersed phase by acetic acid does not necessarily allow the determination of the presence of PMMA dispersed-phase domains with length scales of 20–30 nm or less. This is due to an interfacial PS/PMMA layer formed around the PMMA dispersed phase during melt extrusion; this PS/PMMA interfacial layer has a thickness of ~5 nm at equilibrium [66]. Because acetic acid is not expected to dissolve away the interfacial regions in which PS is present, the etching technique is thus limited in its ability to reveal the presence of very small nanodomains in the blend.) While it is not possible to calculate accurate D_n values for the highly irregularly shaped minor-phase domains in the pulverized blend never subjected to melt processing (Fig. 1a), it appears that there is little growth in the average domain size during the single-screw melt extrusion of the pulverized blend (Fig. 2a). However, because interfacial tension effects are operative during melt extrusion, after melt processing of the pulverized blend the dispersed-phase domains are largely spherical (Fig. 2a), and there is a loss of the somewhat interconnected nature of the minor phase observed in the pulverized blend (Fig. 1a).

Fig. 2a–c illustrates how the morphology of the blend subjected to SSSP followed by short-residence-time single-screw extrusion is affected by high-temperature static annealing. After 10 min annealing at 190 °C, the majority of the dispersed-phase domains have diameters in the range of 300–1000 nm. After 60 min annealing at 190 °C, image analysis of several hundred dispersed-phase domains indicates that $D_n = 1.17$ μm, which is a factor of 7–8 times larger than the value of D_n observed prior to high-temperature static annealing. Thus, while SSSP can be used to produce nanoblends that remain as nanoblends during short-residence-time melt processing, the nanostructured morphology may not be maintained during long-residence-time melt processing allowing for the possibility of significant coarsening.

However, if it is possible to compatibilize the blend during SSSP without significantly affecting the nanostructure development during pulverization, it may then be possible to produce nanoblends via SSSP that maintain nanostructured morphologies during any melt processing to which they are subjected. Previous works by Lebovitz et al. [44,45] have shown that under certain circumstances SSSP can be used to achieve in situ compatibilization of immiscible polymer blends. The SSSP screw design and pulverization conditions (feed rate, screw rotation rate, and screw temperatures) need to be optimized so that both measurable levels of chain scission and sufficiently long-residence times in the pulverizer can be achieved, as both are prerequisites for interpolymer radical coupling reactions leading to block copolymer formation at blend interfaces [45]. With the screw design and pulverization conditions employed in the current study, the pulverized PS/PMMA blend exhibited relatively little chain scission. This is evident from Table 1 which shows the molecular weight averages of the PS and the PMMA in the blends before and after SSSP. Based on the reduction in M_n values after being subjected to SSSP, ~10% of the PS chains and ~30% of the PMMA chains underwent scission during SSSP. The combination of the relatively short-residence-time associated with the SSSP screw design and the modest level of polymer radical formation during SSSP (caused by chain scission accompanying SSSP) is apparently insufficient to yield in situ blend compatibilization.

Recently, we demonstrated that compatibilization of a 90/10 wt% PS/HDPE blend could be achieved by the addition of a commercially available styrene/ethylene–butylene/styrene (SEBS) triblock copolymer to the blend during SSSP [47]. (Without the addition of a triblock copolymer as a compatibilizing agent, the 90/10 wt% PS/HDPE blend exhibited significant coarsening during high-temperature static annealing; the coarsening was nearly eliminated in the blend produced by the addition of 5 wt% SEBS.) Since S/MMA block copolymers are not commercially available (at prices that justify their use in blend processing), we have chosen to use S/MMA gradient copolymers as compatibilizers that can be added to our blend during SSSP. We have recently synthesized S/MMA gradient copolymers using nitroxide-mediated controlled radical polymerization, and we have shown that gradient copolymers can serve as highly effective compatibilizers of microstructured PS/PMMA blends made by melt mixing [53].

The S/MMA gradient copolymer employed in the current study has an apparent M_n of 102,000 g/mol and has 55 mol% S and 45 mol% MMA. The proof of the composition gradient in the gradient copolymer is provided in Fig. 3, where the cumulative styrene mole fraction in the gradient copolymer is observed to decrease as a function of apparent normalized chain length. (The apparent normalized chain length is determined by the ratio of the apparent M_n of the copolymer recovered from a sample aliquot taken at a specific time during the synthesis of the full gradient copolymer to the apparent M_n of the full gradient copolymer.)

Fig. 4 shows the effect of the addition of 5 wt% S/MMA gradient copolymer to the PS/PMMA blend. The micrographs are of blends that were made by SSSP (with gradient copolymer added during SSSP) and then melt processed by short-residence-time single-screw melt extrusion (Fig. 4a) followed by high-temperature static annealing (Fig. 4b and c). Image

Table 1
Molecular weight averages of PS and PMMA before SSSP and after SSSP of an 80/20 wt% PS/PMMA blend

	PS before SSSP	PS after blending via SSSP	PMMA before SSSP	PMMA after blending via SSSP
M_n (g/mol)	116,000	105,000	54,000	41,000
M_w (g/mol)	280,000	273,000	100,000	79,000
PDI	2.4	2.6	1.9	1.9

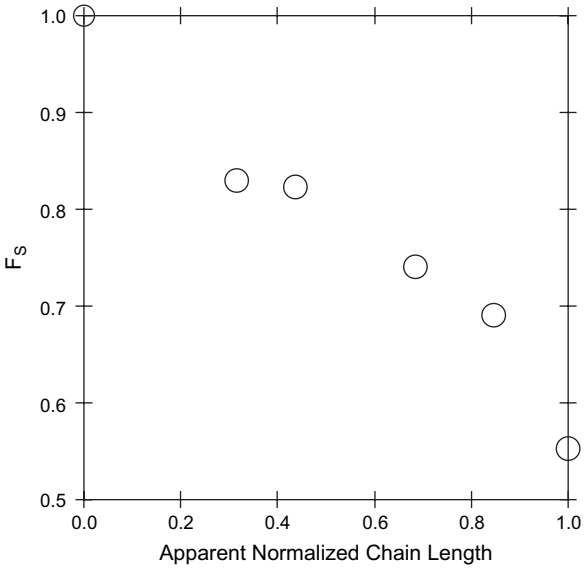

Fig. 3. Cumulative styrene mole fraction (F_S) of S/MMA gradient copolymer as a function of normalized chain length achieved during the synthesis. The evolution of F_S as a function of apparent normalized chain length is proof of the composition gradient achieved along the copolymer chain length.

analysis of several hundred dispersed-phase domains reveals prior to static annealing $D_n = 180$ nm (estimated error of ± 10 nm); this is within $\sim 15\%$ of the value of D_n obtained in the blend lacking gradient copolymer that was subjected to SSSP followed by single-screw extrusion. Thus, the addition of S/MMA gradient copolymer to the PS/PMMA blend during SSSP does little to affect the quasi-nanoscale dispersion achieved in the blend.

However, the addition of the gradient copolymer has a major effect on the coarsening that occurs during high-temperature static annealing. Image analysis of several hundred dispersed-phase domains reveals that $D_n = 245$ nm (± 10 nm) after 60 min static annealing at 190 °C, a 36% increase in D_n due to coarsening that accompanied annealing. In contrast, in the blend made without added gradient copolymer, there was a $\sim 650\%$ increase in D_n due to coarsening that accompanied annealing for 60 min at 190 °C. Thus, the addition of gradient copolymer to the blend during SSSP results in strong suppression of coarsening.

This effect may be quantified by comparing the values of the coarsening rate parameter, K, associated with the following equation [67–69]:

$$D_n^3(t) = D_n^3(0) + Kt \quad (1)$$

where t is annealing time. (We note that our K value differs from that described by Crist and Nesarikar [67] by a factor of 8 due to the fact that our equation involves the cube of the average diameter while their equation involved the cube of the average radius.) Eq. (1) is valid whether the coarsening mechanism is coalescence, Ostwald ripening, or some combination of the two mechanisms. Assuming the simplest of pictures (Brownian motion only) responsible for coarsening by coalescence [67], K is proportional to the quantity Tf/η, where T is the absolute temperature, f is the volume fraction of the dispersed phase, and η is the matrix viscosity. Assuming the simplest of pictures responsible for coarsening by Ostwald ripening [67], K is proportional to the quantity $\mathcal{D}\gamma/T$, where $\mathcal{D}$ is the molecular diffusion coefficient of the dispersed-phase polymer through the matrix polymer and γ is the interfacial energy between the

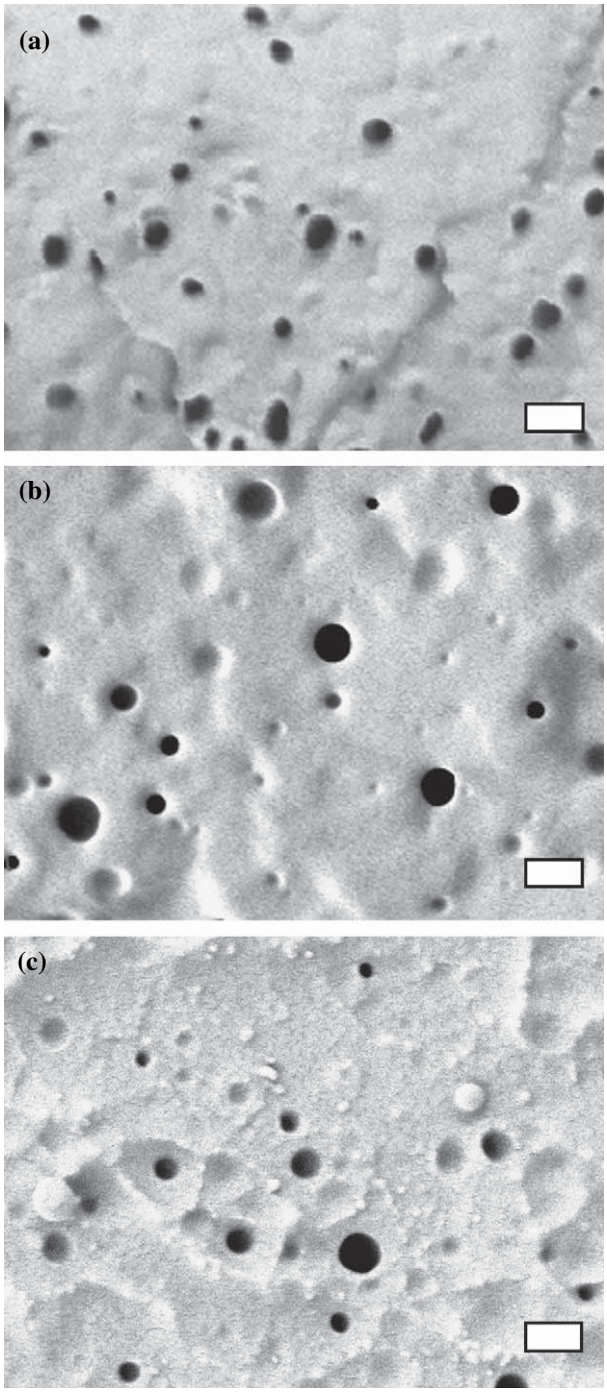

Fig. 4. Scanning electron micrographs of an 80/20 wt% PS/PMMA blend with 5 wt% S/MMA gradient copolymer added during SSSP and then subjected to (a) single-screw melt extrusion, (b) single-screw melt extrusion and static annealing at 190 °C for 10 min, and (c) single-screw melt extrusion and annealing at 190 °C for 60 min. In each case, PMMA was extracted using acetic acid, and the size bar = 500 nm.

two phases. Analysis of our experimental data using Eq. (1) reveals that $K = 2.7 \times 10^{-2}$ μm^3/min in the blends without gradient copolymer, while $K = 1.5 \times 10^{-4}$ μm^3/min in the blends with 5 wt% gradient copolymer. Thus, the addition of gradient copolymer to the blend during SSSP results in a coarsening rate constant that is a factor of 180 smaller than that for the blend made without gradient copolymer. This outcome is somewhat better than the result obtained by Kim et al. [53] upon the addition of S/MMA gradient to a PS/PMMA blend during melt mixing; in that case the coarsening rate constant for the blend with the added gradient copolymer was reduced by a factor of 110 as compared with the blend made without gradient copolymer. Thus, not only is gradient copolymer a highly effective blend compatibilizer, but the use of SSSP as a means of dispersing the gradient copolymer with a goal of achieving blend compatibilization can be as effective if not more so than the use of melt mixing. This means that after processing by SSSP a sufficient quantity of the gradient copolymer is at or near the blend interfaces to yield compatibilization.

In order to determine the effect of polymer material characteristics on the ability of SSSP to yield nanostructured blend morphologies, we also pulverized two other blend systems, PS/PnBMA and PS/HDPE, using exactly the same SSSP screw design, screw speed, and pulverization temperatures employed for the PS/PMMA blends described above. Fig. 5a and b compares the morphologies of 85/15 wt% PS/PnBMA blends made by SSSP (sample experienced room-temperature platen pressing but no melt processing before scanning electron microscopy) and by melt mixing in a minimax mixer with three steel balls. Fig. 5c and d compares the morphologies of 70/30 wt% PS/PnBMA blends made by SSSP (sample experienced room-temperature platen pressing but no melt processing before scanning electron microscopy) and by melt mixing in a minimax mixer with three steel balls. The morphologies developed in the 85/15 wt% and 70/30 wt% blends made by SSSP have similarly sized and irregularly shaped dispersed-phase domains. These dispersed-phase domains, with many having length scales in the range of 300–400 nm, are somewhat larger than those observed in the PS/PMMA blends and thereby disallow the classification of these systems as nanoblends (or blends near the nanoscale border). The absence of a significant dependence of the dispersed-phase domain size on the level of minor phase in the blends made by SSSP was previously reported by Lebovitz et al. [46] in a study of PS/polyethylene (PE) wax blends (with the PE level varying from 1 to 15 wt%). Smith et al. [36] also observed that the length scale of the dispersed phase in blends of poly(ethylene-*alt*-propylene) or polyisoprene with PMMA was largely unaffected by the blend composition when the blends were made by cryogenic ball milling.

In contrast, the 85/15 wt% and 70/30 wt% PS/PnBMA blends made by melt mixing yield much larger dispersed-phase domain sizes than the blends made by SSSP and also exhibit a significant increase in domain size with an increasing level of the minor phase. The increase in domain size with minor-phase content is attributable to the presence of coalescence and Ostwald ripening during the melt mixing; both

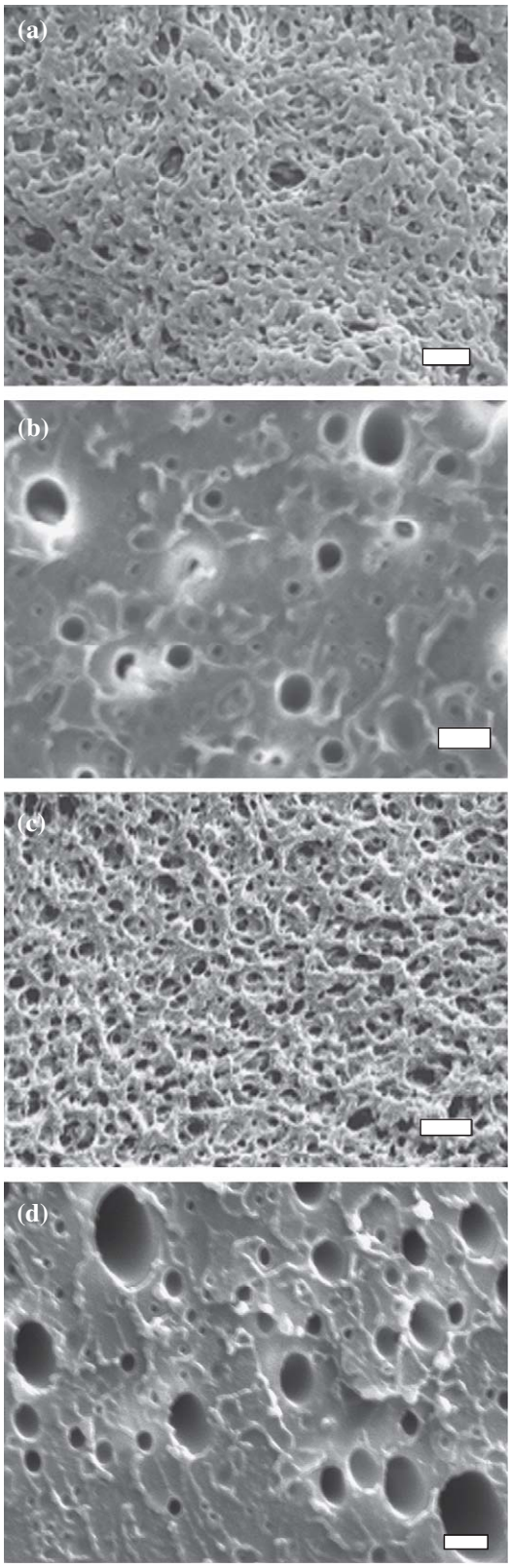

Fig. 5. Scanning electron micrographs of 85/15 wt% PS/PnBMA blends prepared via (a) SSSP followed by platen pressing without melt processing, and (b) melt mixing in a minimax mixer with three steel balls. Scanning electron micrographs of 70/30 wt% PS/PnBMA blends prepared via (c) SSSP followed by platen pressing without melt processing, and (d) melt mixing in a minimax mixer with three steel balls. In (a)–(d), PnBMA was extracted with isopropanol, and the size bar = 2 μm.

coarsening mechanisms will yield larger dispersed-phase domains with increasing dispersed-phase content. As neither coarsening mechanism is present during solid-state processing, there is no significant change in dispersed-phase domain size with minor-phase content during SSSP or cryogenic ball milling of blends.

The results of the 90/10 wt% PS/HDPE blend system were previously reported in Ref. [47]. The microstructure of the PS/HDPE blend system was evaluated by taking the output of the pulverized blend and melt processing it via a short-residence-time single-screw melt extruder. The $D_n(0)$ value obtained in that case was 490 nm [47], small by the standards of conventionally produced, microscale blends but beyond the size scale associated with nanoblends.

Thus, it is apparent that there are significant differences in the length scale associated with the dispersed phase of PS/PMMA, PS/PnBMA, and PS/HDPE blends when they are processed via SSSP using identical screw designs, screw speeds, and temperatures. Why is it that a certain set of SSSP conditions yield a PS/PMMA blend that can be classified either as a nanoblend or a blend near the nanoscale border ($D_n(0) = 155$ nm for an 80/20 wt% PS/PMMA blend without gradient copolymer and $D_n(0) = 180$ nm for an 80/20 wt% PS/PMMA blend with gradient copolymer) while pulverization of PS/PnBMA and PS/HDPE blends under identical conditions yields blends with D_n values of 300–500 nm? At present, we do not have a definitive answer. However, we hypothesize that the nanoscale dispersion achieved in the PS/PMMA blend is attributable in part to the fact that both blend components are deep in the glassy state during pulverization, which may result in a finer dispersion during the repeated fragmentation and fusion steps accompanying SSSP. In contrast, in the other two blends, the dispersed phase is either close to its T_g during SSSP (in the case of PnBMA, $T_g = \sim 15$ °C) or is in a semi-crystalline state with a rubbery amorphous phase during SSSP (in the case of HDPE, its T_g is below 0 °C while its melt transition temperature is well in excess of 100 °C).

Greater study of this issue will be undertaken in the near future. This will involve the study of morphology in other glassy/glassy blends, glassy/near-T_g blends, and glassy/semi-crystalline blends made by SSSP. The roles of SSSP process parameters, including screw design, screw speed, and temperature at various locations along the pulverizer screw, in achieving nanoscale blends will also be investigated.

4. Conclusions

A new process method is demonstrated for achieving nanostructured polymer blends. This approach is based on solid-state shear pulverization, which yields a fine dispersion of a minor phase in a major phase due to repeated fragmentation and fusion steps within the pulverizer; this solid-state process eliminates certain limitations to the production of nanoblends by melt-state processes, e.g., interfacial tension effects leading to coarsening or coalescence. When an 80/20 wt% PS/PMMA blend is made by SSSP, the morphology of the SSSP output is characterized by consolidating the sample by platen pressing (without any melt-state processing) followed by extraction of the PMMA phase and field-emission scanning electron microscopy. This blend exhibits many irregular, minor-phase domains with length scales of ~100 nm or less. When the pulverized blend is subjected to short-residence-time single-screw extrusion, the resulting nanoblend exhibits spherical dispersed-phase domains with $D_n = 155$ nm. Thus, SSSP followed by short-residence-time melt-processing operations can yield products that are nanostructured blends.

However, upon exposure to long-term, high-temperature static annealing, the pulverized blend exhibits significant coarsening of the dispersed-phase domains, meaning that SSSP followed by other melt processes may yield microstructured blends. In order to arrest coarsening, an S/MMA gradient copolymer is synthesized by controlled radical polymerization. When 5 wt% gradient copolymer is added to the PS/PMMA blend during SSSP, the result is a compatibilized nanoblend which exhibits a nanostructure nearly identical to that of the blend without gradient copolymer but with a nearly total suppression of coarsening during high-temperature annealing. Thus, compatibilized nanoblends can be achieved by SSSP combined with gradient copolymer addition. This is one of the first, if not the first, industrially scalable approaches to yield compatibilized, thermoplastic nanoblends that do not rely on in situ polymerization or reactive processing. The morphology of the PS/PMMA blends is also compared to those obtained in other blends subjected to identical SSSP conditions, allowing for commentary on the potential impact of blend components in achieving nanoblend morphologies.

Acknowledgements

The support by Northwestern University, the NSF-MRSEC program (Grant DMR-0076096 and Grant DMR-0520513), and a 3M Fellowship (to JK) is gratefully acknowledged. We also acknowledge the use of field-emission and standard scanning electron microscopes in a shared user facility of the Northwestern University Materials Research Center. We also thank Prof. SonBinh Nguyen and Dr. Hongying Zhou for the synthesis of alkoxyamine 29 that was originally used in Refs. [53,55].

References

[1] Harrats C, Thomas S, Groeninckx G. Micro- and nanostructured multiphase polymer blend systems: phase morphology and interfaces. New York: Taylor & Francis; 2006.
[2] Banerjee P, Mandal BM. Macromolecules 1995;28:3940–3.
[3] Yang CY, Hide F, Heeger AJ, Cao Y. Synth Met 1997;84:895–6.
[4] Smith AP, Bai C, Ade H, Spontak RJ, Balik CM, Koch CC. Macromol Rapid Commun 1998;19:557–61.
[5] Smith AP, Spontak RJ, Ade H, Smith SD, Koch CC. Adv Mater 1999;11:1227–81.
[6] Hu GH, Cartier H, Plummer C. Macromolecules 1999;32:4713–8.
[7] Dreezen G, Ivanov DA, Nysten B, Groeninckx G. Polymer 2000;41:1395–407.
[8] Pernot H, Baumert M, Court F, Leibler L. Nat Mater 2002;1:54–8.
[9] Kietzke T, Neher D, Landfester K, Montenegro R, Guntner R, Scherf U. Nat Mater 2003;2:408–12.

[10] Iyengar NA, Harrison B, Duran RS, Schanze KS, Reynolds JR. Macromolecules 2003;36:8978–85.
[11] Hu GH, Feng LF. Macromol Symp 2003;195:303–8.
[12] Chan SH, Lin YY, Ting C. Macromolecules 2003;36:8910–2.
[13] Busby AJ, Zhang JX, Naylor A, Roberts CJ, Davies MC, Tendler SJB, et al. J Mater Chem 2003;13:2838–44.
[14] Akiba I, Masunaga H, Sasaki K, Shikasho K, Sakurai K. Polymer 2004; 45:5761–4.
[15] Apostolo M, Triulzi F. J Fluorine Chem 2004;125:303–14.
[16] Prosycevas I, Tamulevicius S, Guobiene A. Thin Solid Films 2004;453: 304–11.
[17] Kailas L, Audinot JN, Migeon HN, Bertrand P. Appl Surf Sci 2004;231: 289–95.
[18] Yamazaki M, Kayama M, Ikeda K, Alii T, Ichihara S. Carbon 2004;42: 1641–9.
[19] Ji YL, Li WG, Ma JH, Liang BR. Macromol Rapid Commun 2005;26: 116–20.
[20] Leibler L. Prog Polym Sci 2005;30:898–914.
[21] Shimizu H, Li YJ, Kaito A, Sano H. Macromolecules 2005;38:7880–3.
[22] Alam TM, Otaigbe JU, Rhoades D, Holland GP, Cherry BR, Kotula PG. Polymer 2005;46:12468–79.
[23] Freemantle M. C&E News 2002;80(36):12.
[24] Koning C, van Duin M, Pagnoulle C, Jerome R. Prog Polym Sci 1998;23: 707–57.
[25] Matos M, Favis BD, Lomellini P. Polymer 1995;36:3899–907.
[26] Fortelny I. In: Harrats C, Thomas S, Groeninckx G, editors. Micro- and nanostructured multiphase polymer blend systems: phase morphology and interfaces. New York: Taylor & Francis; 2006. p. 43–90.
[27] Sundararaj U. In: Harrats C, Thomas S, Groeninckx G, editors. Micro- and nanostructured multiphase polymer blend systems: phase morphology and interfaces. New York: Taylor & Francis; 2006. p. 133–64.
[28] Favis BD. Formulations. In: Paul DR, Bucknall CB, editors. Polymer blends, vol. 1. New York: Wiley; 2000. p. 501–37.
[29] Utracki LA, Shi ZH. Polym Eng Sci 1992;32:1824–33.
[30] Tucker CL, Moldenaers P. Annu Rev Fluid Mech 2002;34:177–210.
[31] Grace HP. Chem Eng Commun 1982;14:225–77.
[32] Taylor GI. Proc R Soc London Ser A 1934;146:501–23.
[33] Sundararaj U, Macosko CW. Macromolecules 1995;28:2647–57.
[34] Wu SH. Polym Eng Sci 1987;27:335–43.
[35] Smith AP, Spontak RJ, Koch CC, Smith SD, Ade H. Macromol Mater Eng 2000;274:1–12.
[36] Smith AP, Ade H, Balik CM, Koch CC, Smith SD, Spontak RJ. Macromolecules 2000;33:2595–604.
[37] Martin JP, McCartney SR, Kander RG. J Mater Sci 2003;38:195–200.
[38] Stranz M, Koster U. J Mater Sci 2004;39:5275–7.
[39] Chen Z, Wang Q. Polym Int 2001;50:966–72.
[40] Khait K, Torkelson JM. Polym Plast Technol Eng 1999;38:445–57.
[41] Furgiuele N, Lebovitz AH, Khait K, Torkelson JM. Macromolecules 2000;33:225–8.
[42] Furgiuele N, Lebovitz AH, Khait K, Torkelson JM. Polym Eng Sci 2000; 40:1447–57.
[43] Khait K, Torkelson JM. Int Polym Proc 2000;15:343–7.
[44] Lebovitz AH, Khait K, Torkelson JM. Macromolecules 2002;35:8672–5.
[45] Lebovitz AH, Khait K, Torkelson JM. Macromolecules 2002;35:9716–22.
[46] Lebovitz AH, Khait K, Torkelson JM. Polymer 2003;44:199–206.
[47] Tao Y, Lebovitz AH, Torkelson JM. Polymer 2005;46:4753–61.
[48] Brinker KL, Lebovitz AH, Torkelson JM, Burghardt WR. J Polym Sci Part B Polym Phys 2005;43:3413–20.
[49] Matyjaszewski K, Ziegler MJ, Arehart SV, Greszta D, Pakula T. J Phys Org Chem 2000;13:775–86.
[50] Qin SH, Saget J, Pyun JR, Jia SJ, Kowalewski T, Matyjaszewski K. Macromolecules 2003;36:8969–77.
[51] Gray MK, Zhou HY, Nguyen ST, Torkelson JM. Polymer 2004;45: 4777–86.
[52] Gray MK, Zhou HY, Nguyen ST, Torkelson JM. Macromolecules 2004; 37:5586–95.
[53] Kim J, Gray MK, Zhou HY, Nguyen ST, Torkelson JM. Macromolecules 2005;38:1037–40.
[54] Woo D, Kim J, Suh MH, Zhou HY, Nguyen ST, Lee SH, et al. Polymer 2006;47:3287–91.
[55] Kim J, Zhou HY, Nguyen ST, Torkelson JM. Polymer 2006;47: 5799–809.
[56] Lefay C, Charleux B, Save M, Chassenieux C, Guerret O, Magnet S. Polymer 2006;47:1935–45.
[57] Karaky K, Pere E, Pouchan C, Garay H, Khoukh A, Francois J, et al. New J Chem 2006;30:698–705.
[58] Major MD, Torkelson JM, Brearley AM. Macromolecules 1990;23: 1711–7.
[59] Shull KR. Macromolecules 2002;35:8631–9.
[60] Lefebvre MD, Dettmer CM, McSwain RL, Xu C, Davila JR, Composto RJ, et al. Macromolecules 2005;38:10494–502.
[61] Benoit D, Chaplinski V, Braslau R, Hawker CJ. J Am Chem Soc 1999; 121:3904–20.
[62] Lebovitz AH. Ph.D. thesis, Northwestern University; 2003.
[63] Maric M, Macosko CW. Polym Eng Sci 2001;41:118–30.
[64] Lee MS, Lodge TP, Macosko CW. J Polym Sci Part B Polym Phys 1997; 35:2835–42.
[65] Macosko CW, Guegan P, Khandpur AK, Nakayama A, Marechal P, Inoue T. Macromolecules 1996;29:5590–8.
[66] Anastasiadis SH, Russell TP, Satija SK, Majkrzak CF. Phys Rev Lett 1989;62:1852–5.
[67] Crist B, Nesarikar AR. Macromolecules 1995;28:890–6.
[68] Song SW, Torkelson JM. J Membr Sci 1995;98:209–22.
[69] Siggia ED. Phys Rev A 1979;20:595–605.